HER⬤N

Contents

COMPUTER SIMULATION OF THE
E.C.C.S. BUCKLING CURVE USING A
MONTE-CARLO METHOD

John Strating
Han Vos
(STEVIN LABORATORY,
DELFT UNIVERSITY OF
TECHNOLOGY)

COMPUTER SIMULATION OF THE E.C.C.S. BUCKLING CURVE USING A MONTE-CARLO METHOD

Abstract

The application of a Monte-Carlo simulation procedure to obtain the distribution function of the maximum load of a hinged column with imperfections is discussed. Buckling tests carried out by the E.C.C.S. on IPE 160 sections have been simulated. Information concerning the column variables is obtained from the data-sheets of the E.C.C.S. tests. The probability density function of each variable is derived or estimated. A good agreement is found between the simulated buckling curve and the experimental buckling curve.

Acknowledgement

3

Computer simulation of the E.C.C.S. buckling curve using a Monte-Carlo method

1 Introduction

This paper describes a procedure for computer simulation of buckling tests, using a Monte-Carlo method. The variation of the parameters which determine the load-carrying capacity of a column is taken into account and the probability density-function of the buckling load is derived.

In the past years, the European Convention for Constructional Steelwork (E.C.C.S.) has carried out an extensive experimental programme on buckling of concentrically loaded, hinged columns with imperfections. The results of these tests are discussed in [1]. Most specimens tested were light-weight sections with flange thicknesses $e \leqslant 20$ (mm). The test series has been designed in such a way that a buckling curve with a certain probability of failure could be derived. The buckling curve is defined by means of characteristic stresses. According to the philosophy of the E.C.C.S., the characteristic buckling stress σ_{CR}^{*} is equal to

$$\sigma_{CR}^{*} = m - k \cdot s$$

where m is the mean value and s is the standard deviation of the buckling stresses; k is a constant which depends on the type of probability density function (p.d.f.) of σ_{CR}.

The value of k must be chosen so that: prob. $[\sigma_{CR} \leqslant \sigma_{CR}^{*}]$ is equal to 2.3%. If σ_{CR} follows a Gaussian p.d.f. the value of $k = 2$.

Information concerning the type of p.d.f. of buckling stresses could be obtained only through experiments at the time the E.C.C.S. tests were started.

The number of tests involved is large, however. The p.d.f. is estimated from the results.

As shown in [1], the shape of the experimental buckling curve is determined mainly by the test results on IPE 160 sections. The buckling curve is shown in (Fig. 1) together with the significant test results. A statistical analysis of the buckling stresses proved that the buckling stresses are Gaussian distributed and therefore

$$\sigma_{CR}^{*} = m - 2 \cdot s$$

Due to the great number of tests involved in the above-mentioned approach, it cannot be extended easily to all the various sectional shapes and dimensions. Neither time nor means are available to carry out these tests.

Theoretical solutions are sought, therefore which are able to predict the behaviour

5
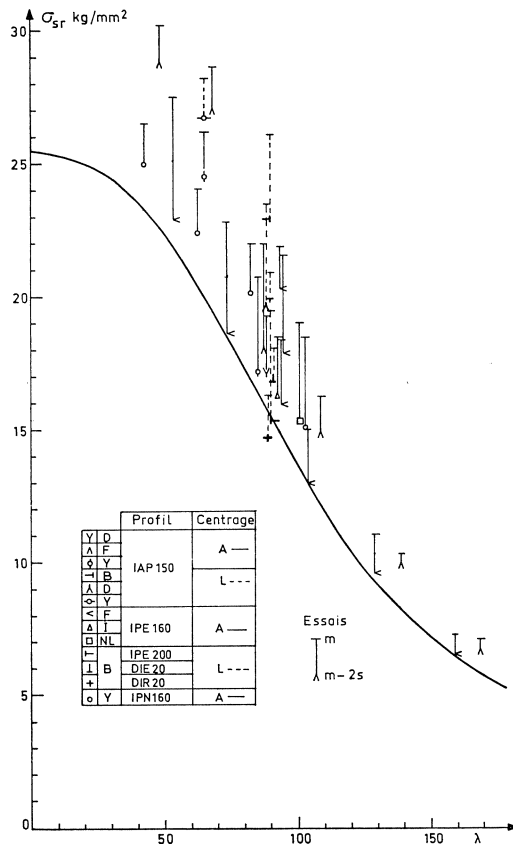
Fig. 1

of an imperfect column with sufficient accuracy and which also take into account the random nature of the imperfections and the mechanical properties. Two problems can be recognized which must be solved.

1. To compute the buckling load of a concentrically loaded column, given certain imperfections and mechanical properties.
2. To compute the probability density-function of the buckling loads or stresses, given the imperfections and mechanical properties are random variables.

It is obvious that the first problem must be solved before the second problem can be tackled. Batterman and Johnston [2]. Stüssi [3], as well as Beer and Schulz [4] have discussed numerical methods for solving the case of a concentrically loaded column with certain imperfections. These methods are used to carry out the computations involved in the outlined procedure and they will be discussed briefly in chapter 3.

6

This paper is concerned primarily with the solution of the second problem, however. A Monte-Carlo simulation procedure is applied to derive the p.d.f. of the buckling stresses. The results of the E.C.C.S.-tests on IPE specimens are analysed and used to check the validity and accuracy of this kind of approach. Information concerning the imperfections and mechanical properties of these sections has been obtained from the data sheets which were established for each test specimen. The p.d.f.'s of the column variables can be derived from this information. These functions are used as input-sources for the Monte-Carlo simulation procedure.

Finally, a buckling curve is computed with known probability of failure. This curve compares well with the experimental E.C.C.S. buckling curve derived from the same specimens.

2 Computer simulation of buckling curves

The buckling load of a hinged column with imperfections can be described by the following relation

$$P_{CR} = f(\sigma_{yt}, \sigma_{yc}, \sigma_r, e_0, f_0, A, E, \lambda)$$

where σ_{yt} = yield stress in tension
σ_{yc} = yield stress in compression
σ_r = residual stress
e_0 = eccentricity
f_0 = amplitude of the initial curvature
A = area
E = Young's modulus
λ = slenderness-ratio

It should be emphasized that the variables which appear in this relation are random variables. The number of variables can be reduced if σ_{yt} is assumed to be equal to σ_{yc}, and that E is constant; the relation can then be written as

$$P_{CR} = f(\sigma_y, \sigma_r, e_0, f_0, A, \lambda).$$

Proof of the influence of each variable on the scatter of the buckling load P_{CR} can be obtained through correlation analysis of tests results, as shown by Loof for the E.C.C.S. tests [5].

According to the criteria of the E.C.C.S., the characteristic buckling load is equal to

$$P_{CR}^* = \bar{P}_{CR} - k \cdot s$$

P_{CR}^* = characteristic value of the buckling load
$\bar{P}_{CR}$ = mean value of the buckling load
s = standard deviation of the buckling load
k = constant such that prob $[P_{CR} \leqslant P_{CR}^*] = 2.3\%$

It is obvious that the value of k depends on the type of p.d.f. of P_{CR}. A value for P_{CR}^* can be determined, without much difficulties, from experiments. A theoretical solution for P_{CR}^*, is much more difficult to obtain, however. P_{CR} is a function of a number of random variables, consequently P_{CR} follows a multi-dimensional probability density-function. This function is not known generally nor can this function be derived from information concerning the p.d.f.'s of the random variables, except in a few special cases. A purely theoretical solution of the problem in question is not feasible therefore in most cases. Two approximate solutions, however, have been suggested; they are discussed below and a new approach is described.

2.1 *Method I*

Various combinations of the variables are introduced into the formula for P_{CR}. Each combination leads to another buckling curve (varying λ). By comparing the computed buckling curve with the experimental E.C.C.S. buckling curve, a combination of variables can be estimated which fits the experimental curve most closely over the whole range of slenderness-ratios. This method has been adopted and developed by Beer and Schulz [4] .From a probabilistic point of view, this method is questionable because a lower bound curve is approximated. There is no reason to assume that the obtained solution is unique.

Extrapolation to other shapes and dimensions is realised by modifying the combination of the variables. No information concerning the scatter in the buckling loads is obtained, however. This method is therefore not truly probabilistic.

2.2 *Method II*

Schor [6] and Carpena [1] assume that all variables are uncorrelated, and furthermore that the function $f(\sigma_y, \sigma_r, e_0, f_0, A, \lambda)$, can be linearized. A linear function is obtained through a Taylor expansion of f

$$f(\sigma_y, \sigma_r, e_0, f_0, A, \lambda) = f(\bar{\sigma}_y, \bar{\sigma}_r, \bar{e}_0, \bar{f}_0, \bar{A}, \lambda) + \frac{\partial_f}{\partial \sigma_y}(\sigma_y - \bar{\sigma}_y) +$$

$$+ \frac{\partial_f}{\partial \sigma_r}(\sigma_r - \bar{\sigma}_r) + \frac{\partial_f}{\partial e_0}(e_0 - \bar{e}_0) + \frac{\partial_f}{\partial f_0}(f_0 - \bar{f}_0) + \frac{\partial_f}{\partial A}(A - \bar{A}) +$$

$$+ \frac{\partial_f^2}{\partial \sigma_y^2}\frac{(\sigma_y - \bar{\sigma}_y)^2}{2!} + \frac{\partial_f^2}{\partial \sigma_r^2}\frac{(\sigma_r - \bar{\sigma}_r)^2}{2!} + \dots$$

Disregarding all terms of the second order and higher, the expansion reduces to

$$f(\sigma_y, \sigma_r, e_0, f_0, A, \lambda) \approx f(\bar{\sigma}_y. \bar{\sigma}_r, \bar{e}_0, \bar{f}_0, \bar{A}, \lambda) + \frac{\partial_f}{\partial \sigma_y}(\sigma_y - \bar{\sigma}_y) +$$

$$+ \frac{\partial_f}{\partial \sigma_r}(\sigma_r - \bar{\sigma}_r) + \frac{\partial_f}{\partial e_0}(e_0 - \bar{e}_0) + \frac{\partial_f}{\partial f_0}(f_0 - \bar{f}_0) + \frac{\partial_f}{\partial A}(A - \bar{A}).$$

The mean value of P_{CR} can be found by substituting $(\bar{\sigma}_y, \bar{\sigma}_r, \bar{e}_0, \bar{f}_0, \bar{A})$ into this formula

$$\bar{P}_{CR} \approx f(\bar{\sigma}_y, \bar{\sigma}_r, \bar{e}_0, \bar{f}_0, \bar{A}, \lambda).$$

The variance of P_{CR}, after squaring and summing, is equal to

$$s_p^2 \approx \left(\frac{\partial_f}{\partial\sigma_y} s_y\right)^2 + \left(\frac{\partial_f}{\partial\sigma_r} s_r\right)^2 + \left(\frac{\partial_f}{\partial e_0} s_e\right)^2 + \left(\frac{\partial_f}{\partial f_0} s_f\right)^2 + \left(\frac{\partial_f}{\partial A} s_A\right)^2$$

where s_p = standard deviation of P_{CR}
s_y = standard deviation of σ_y
s_r = standard deviation of σ_r
s_e = standard deviation of e_0
s_f = standard deviation of f_0
s_A = standard deviation of A

It is now possible to compute the mean value of P_{CR} and the variance at each slenderness-ratio λ, provided function $f(\sigma_y, \sigma_r, e_0, f_0, A, \lambda)$ can be solved. The mean values and variances of each variable must also be known. The first derivatives of f can be obtained analytically, by partial differentiation of f or graphically from curves showing the dependance of f upon each variable. If furthermore is assumed that P_{CR} follows a Gaussian p.d.f., the desired buckling curve can be derived by computing for each λ the value $(\bar{P}_{CR} - 2s_p)$.

Essential in the above-mentioned approach are the assumptions that the variables are uncorrelated and that function f can be linearized. The latter assumption must be viewed with reserve and may lead to significant errors.

The described approach can be checked against the E.C.C.S. buckling curve. The mean values and the variances of the variables can be obtained from the data-sheets available for each test specimens. Comparison of the computed buckling curve and the experimental buckling curve will show whether the linearization of f is allowed.

This method itself is basically a probabilistic approach and therefore in agreement with the criteria of the E.C.C.S.

2.3 *Method III*

Carrying out a buckling test simply means loading a column, with a certain combination of imperfections and mechanical properties, until failure occurs. The values of the imperfections and the mechanical properties of a particular column cannot be predicted in advance.

Once a column has been selected for a test, however, these values can be measured. If the mathematical model of such a column is sufficiently accurate, the buckling load of this column can be computed instead of actually carrying out a buckling test. This can be repeated for any number of columns. None of the columns are actually tested, all buckling loads are computed, the tests are "simulated". The simulation

method can be further generalized if it is recognized and acknowledged that the values of the imperfections and the mechanical properties present in a column are primarily due to chance. It is sufficient to know the distribution function of each variable and the correlations between these variables, to carry out the simulation procedure. One drawing from the population of each variable, giving proper attention to the correlations between them, results in a combination of variables which can be assigned to a hypothetical column; the buckling load P_{CR} of this hypothetical column can then be computed. If this procedure is repeated a number of times, an equal number of P_{CR} values is obtained. The mean value as well as the variance of P_{CR} can be determined and a p.d.f. can be fitted to the histogram of P_{CR}-values. By doing this, the E.C.C.S. testing procedure is exactly simulated. It is very important of course, to select proper values for each variable. This can be done correctly by deriving the p.d.f.'s of the variables from representative data. A simulation procedure as described above is called a "Monte-Carlo" method. This method is particularly suited for a digital computer because numerous repeated computations are involved.

Drawing values from a particular p.d.f. can be done by generating random numbers which follow the same distribution law as the variable in question. This method allows for correlation of any kind to be introduced between the variables.

The validity of a Monte-Carlo simulation procedure will be tested by applying it to the E.C.C.S. tests carried out on IPE 160 sections. The data-sheets of these tests allow the derivation of most p.d.f.'s involved. The computed buckling curve can be compared directly with the experimental buckling curve because the shape of the latter curve is determined completely by the test results obtained on the IPE 160 specimens. Application of the discussed method to other sections simply means modifying the p.d.f.'s of the variables so that they correspond to these sections.

No buckling tests have to be carried out, only simple measurements are necessary to determine the representative values of the imperfections and the mechanical properties. These measurements are less expensive, however.

The application of the Monte-Carlo simulation method to the E.C.C.S. buckling tests on IPE 160 specimens is discussed in chapters 4, 5 and 6.

3   Numerical solutions for the buckling load of a column with imperfections

Most solutions for the buckling load of a column with imperfections are based on numerically solving the equation which describes the state where in each point of a column the external moment M_{ex} is equal to the internal moment M_i (Fig. 2)

$$P \cdot y = -EI_x \frac{d^2 y}{dx^2}$$

For a given value of P, the deflected shape of the column is assumed: $y = f(x)$. The external moments are computed and are assumed to be equal to the internal moments. Next the shape of the column corresponding to these internal moments is determined.

P is equal to the buckling load of the column if and only if the computed shape of the deflection curve is identical to the assumed one. This is generally not the case and therefore the computation of the deflected shape is repeated starting, however, with the shape obtained in the first computation. It has been shown by various authors that this procedure is rapidly converging and that a sufficiently accurate value of P will be obtained after only a few iteration steps [3, 4].

Next consider the column shown in (Fig. 2). This column is identical to a column with hinged ends and twice its length. A load P is applied to this column with an eccentricity e_0; the column is assumed to have an initial curvature which is part of a sinewave, the amplitude is f_0.
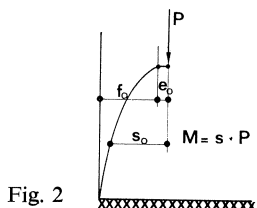
Fig. 2

As a first approximation the deflected shape of this column is also assumed to be a sinewave, the end-deflection of the column is equal to "a". The column is divided into a number of segments. The external bending moments are determined at the ends of each segment. The deflections of the column are computed numerically, by means of the reduced moment-area method and applying Simpson's rule.

For each segment the angle of rotation is computed; the deflection at the top of the column is equal to the sum of the products of the angles of rotation and the segment lengths. The computations are repeated until the computed shape is identical to the assumed shape.

In this iteration process the computed column shape of each previous step is used for the next step. The iteration is stopped if a certain degree of accuracy is obtained between two successive shapes. It is not yet necessary, however, that the computed end-deflection of the column is equal to the assumed end-deflection "a". There are two methods which can be used to bring those two deflections into agreement. In the first method, the value of P is kept constant; the length of the column, however, is varied until both deflections are equal. Next other values of "a" are adopted and for each "a" a corresponding column length (or slenderness-ratio λ) is computed. From these pairs of values (λ, a), the maximum column length is determined for which the given column will be in equilibrium under the load P (Fig. 3). Then the value of P is varied and the computations are repeated. To each value of P there corresponds a maximum column length 1 (or λ_{max}). In the second method the length of the column is kept constant, the value of P is varied until a value is found for which the assumed deflection is equal to the computed deflection. Next "a" is varied and other values of P are found. From the pairs of values (P, a) the collapse load of a column of given length is determined (Fig. 4).

11

Fig. 3

Fig. 4

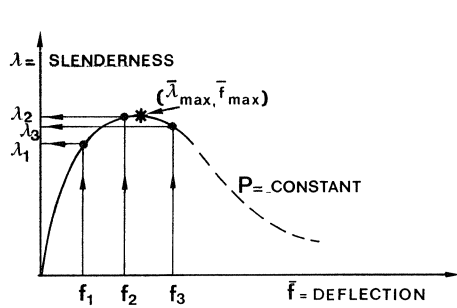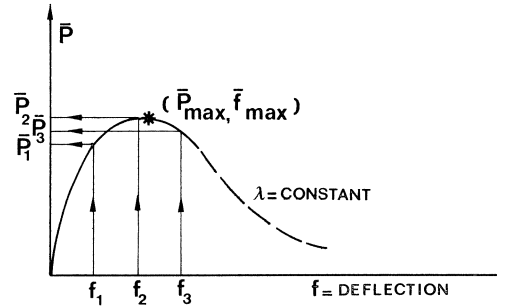The first method has been used by Beer and Schulz for their computations [4]. They were interested in determining complete buckling curves for each combination of variables. The maximum length of a column, for any given value of P, is less interesting for the Monte-Carlo simulation procedure because a column is never tested by increasing the column length during the test until failure occurs. Therefore the second method has been applied. For each column of given length and given imperfections, the critical load P_{CR} is computed.

The computation of the deflected shape of a column is rather complicated because the bending stiffness "EI_x" of the column is not a constant but appears to be a function of the bending moment M and the load P. The column will yield over part of the cross-section, if P is large or if the deflections are large. The bending stiffness "EI_x" will be reduced, due to this yielding. Residual stresses present in the column cause premature yielding. The value of the yield stress and the dimensions of the section will also affect the relations between M, P and EI. The bending moment is not constant over the length of the column, and consequently the bending stiffness EI varies over the column length. The relations between M, P and EI can be determined for each particular section if the stress-strain diagram, the distribution of σ_y over the cross-section and the residual stress distribution are known. For a constant value of P, an increasing part of the cross-section is assumed to yield, the corresponding stress and strain distributions allow the values of the bending moment M and the curvature to be computed. For an IPE 160 section these relations are shown in (Fig. 5). The dimensions of this section are nominal, the stress-strain diagram is assumed to be bi-linear and $\sigma_y = 24.0$ kgf/mm^2. The residual stress is assumed to be parabolically distributed in the flanges and constant in the web; the maximum compressive residual stress is equal to $0.3\sigma_y$. On the vertical axis of figure 5 the ratio $\bar{B}$ between the actual bending stiffness and the elastic bending stiffness is plotted; on the horizontal axis the ratio $\bar{M}$ between the actual bending moment and the plastic bending-moment is plotted. These curves provide the information necessary for the computation of the buckling loads.

From the remarks above it can be observed that the column parameters can be divided into two groups. The yield stress, residual stress and the dimensions affect

12
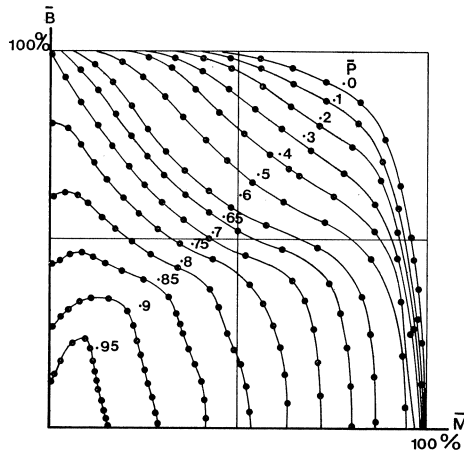
Fig. 5

M̄-B̄-P̄ RELATIONS FOR A IPE 160 SECTION
WEAK-AXIS a=5, b=82, h=160, e=7.4, σ_y=24
ly=683000 α=-.3

the shape of the $\overline{M} - \overline{P} - \overline{B}$ relations while the eccentricity and the initial curvature affect the deflected shape through the external bending moment.

All the column computations which will be discussed in a later chapter, have been carried out under the following assumptions: the stress-strain diagram is bi-linear; the yield stress is constant over the cross-section; the residual stress distribution is parabolic in the flanges and constant in the web, the distribution is symmetric; the initial curvature is half a sinewave and the eccentricity is constant over the length of the column. Only weak-axis buckling is considered. It should be mentioned that the computations involved in the Monte-Carlo simulation procedure are rather tedious because for each column a new set of $\overline{M} - \overline{P} - \overline{B}$ relations must be determined.

The accuracy of the computer programme is checked by comparing the output

$\bar{\lambda}$	α	$\bar{\sigma}$	
		this programme	Beer and Schulz[1])
0.594	0	0.87	0.89
	0.5	0.77	0.78
0.810	0	0.78	0.79
	0.5	0.64	0.65
1.025	0	0.65	0.65
	0.5	0.53	0.53
1.132	0	0.58	0.59
	0.5	0.47	0.47
1.400	0	0.42	0.43
	0.5	0.36	0.35
1.725	0	0.30	0.29
	0.5	0.26	0.25

[1]) These values are obtained from [4] p. 40, fig. 5 and [12] p. 115, fig. 5.6.

with results obtained by Beer and Schulz on a similar column. This comparison is shown in the table below. The column is a HEA 200; the initial curvature $f_0 = l/1000$, the maximum compressive residual stress is 0 or $0.5\sigma_y$, the column dimensions are nominal. The slenderness-ratio and the critical stress are given as dimensionless parameters

$$\bar{\lambda} = \frac{\lambda}{\pi} \sqrt{\frac{\sigma_y}{E}} \quad \text{and} \quad \bar{\sigma} = \frac{\sigma_{CR}}{\sigma_y}$$

4 Column data

A considerable number of the E.C.C.S. buckling tests has been carried out on IPE sections. These sections are responsible for the shape of the experimental buckling curve as derived by the E.C.C.S. It is for this reason that these sections are chosen for the Monte-Carlo simulation procedure.

The testing procedure, established by committee 8.1* of the E.C.C.S., demanded that the following measurement be carried out on each test specimen

1. The dimensions of the specimen at 0, $\frac{1}{4}l$, $\frac{1}{2}l$, $\frac{3}{4}l$, l
2. The initial curvature at $\quad\quad\quad$ 0, $\frac{1}{4}l$, $\frac{1}{2}l$, $\frac{3}{4}l$, l
3. Weighing of the specimen

The mechanical properties of each bar from which specimens were cut had to be determined

4. Tensile tests
5. Stub-column test

These data had to be recorded on a standard data sheet.

In the next paragraphs the relations between the column variables and the measurements are discussed.

4.1 *Eccentricity*

The dimensions of the sections are used to compute the eccentricity which is introduced because the testing procedure requires that the load must be applied at the center of the web of the specimen. The center of the web, however, does not necessarily coincide with the center of gravity of the whole section.

The center of the web lies a distance $(c + \frac{1}{2}a)$ from the right. The center of gravity of the flange lies $\frac{1}{2}b$ from the right. The difference between the two distances is equal to: $(c + \frac{1}{2}a) - \frac{1}{2}b$.

The center of gravity of the complete section is determined for the nominal area.

---

* Committee 8.1 on "Buckling tests".

The eccentricity of the web is computed from the following relation

$$e_0 = \frac{2A_F}{A_n}[c + \tfrac{1}{2}a - \tfrac{1}{2}b]$$

where A_F = area of a flange
A_n = nominal area

If both flanges are considered separately e_0 is equal to

$$e_0 = \frac{A_{F1} + A_{F2}}{2A_n}[(c_1 + \tfrac{1}{2}a_1 - \tfrac{1}{2}b_1) + (c_2 + \tfrac{1}{2}a_2 - \tfrac{1}{2}b_2)]$$

The mean values of the dimensions, determined over the length of the column, are introduced into this formula.
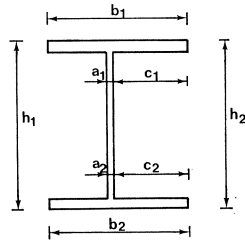
4.2 *Initial curvature*

The initial out-of straightness has been measured at five points along the length of a specimen. A digital computer is used to find the best fit of a sinewave through the points A, B, C, D and E. The amplitude f_0 of the sinewave is considered as the parameter of the initial curvature. The mean value of f_0 for both flanges is determined.
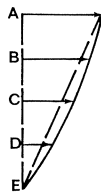
4.3 *Area*

The weight G of a specimen is used to compute the real area of the section. The specific weight of steel is assumed to be

$$\varrho = 7.85 \times 10^{-6} \text{ kgf/mm}^3$$

15

The area is equal to

$$A = \frac{G}{\varrho \cdot l}$$

l = length
ϱ = specific weight
G = weight of the specimen
A = area

4.4 Tensile tests

Tensile tests were executed on specimens taken from the flanges, according to Euronorm 2–57. The yield stress obtained from these tests is denoted σ_{ye}.

Additional tensile tests were carried out on strips taken from the flanges and the web. This yield stress is denoted σ_{ys}. The figures below show how the specimens are taken from the bar.

EURONORM STRIPS
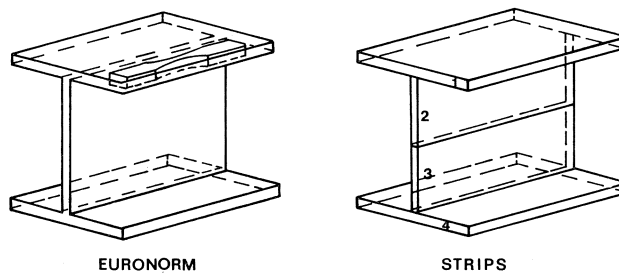
4.5 Stub column test

Stub column tests were carried out on specimens with slenderness-ratios $\lambda = 12$, 15 and 20. The specimens were taken from the same length of bar from which specimens were cut for the buckling tests. The yield stress obtained from these tests is called σ_y.

The individual column data are not reproduced in this paper because they are too numerous. In the next chapter histograms of these data are given, however. The data have been reduced according to the relations given in the previous paragraphs.

The IPE 160 sections studied in this investigation are coded 17, 18, 19, 20, 21 and 22 in Table A-1, page 30 of ref. [1]. The eccentricity and initial curvature parameters are obtained from 150 columns; the yield stresses and areas are obtained from 189 columns.

5 Probability density functions of the column variables

The experimental data described in chapter 4 have been used to derive histograms and cumulative histograms. Cumulative distribution functions are fitted to the cumulative histograms. Throughout this chapter, the Kolmogorov-Smirnov test of signi-

ficance is applied to find the best fit [7], except for the initial curvature. The Kolmogorov-Smirnov test concentrates on the deviations between the hypothesized cumulative distribution function $F(x)$ (C.D.F.) and the observed cumulative histogram $F^*(x_i)$ (C.H.).

$F^*(x_i) = i/n$ where x_i is the i-th largest observed value in a random sample of size n.

The following statistic is considered

$$D = \max_{i=1}^{n} [F^*(x_i) - F(x)]$$

D is, according to this formula, the largest of the absolute values of the differences between the hypothesized C.D.F. and the observed C.H., evaluated at the observed values in the sample. Critical values of D can be given at various levels of significance which will result in either accepting or rejecting the hypothesized C.D.F. Let α be the level of significance, then for large n, the critical statistic is equal to

$$\alpha = 0.10 \qquad \bar{D} = 1.22/\sqrt{n}$$
$$\alpha = 0.05 \qquad \bar{D} = 1.36/\sqrt{n}$$
$$\alpha = 0.01 \qquad \bar{D} = 1.63/\sqrt{n}$$

5.1 *Eccentricity*

The histogram of e_0 is shown in (Fig. 6). The eccentricity varies between 0 and 2.0 mm.

Fig. 6   ECCENTRICITY e_0 mm

17
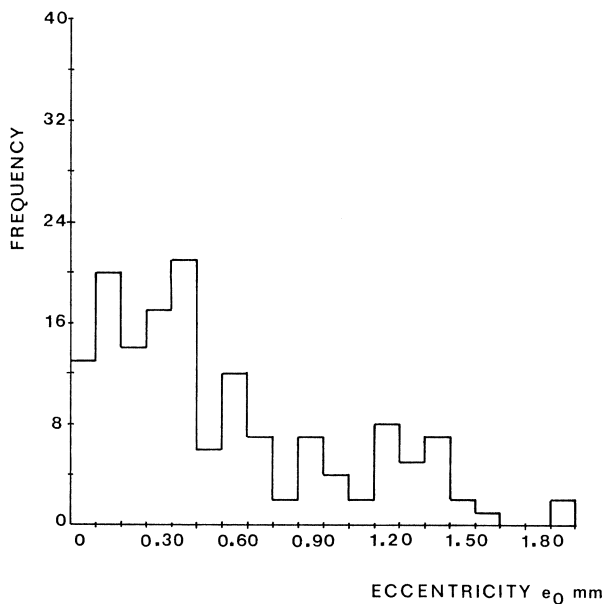
The shape of the histogram suggests an asymmetrical p.d.f. Three C.D.F.'s are hypothesized

a Gaussian   C.D.F.

a Log-normal C.D.F.

a Gamma   C.D.F.

In Fig. 7 the observed C.H. is shown together with the hypothesized C.D.F.'s. The maximum values of D which can be derived from this figure are

$$\text{Gaussian}\quad\text{C.D.F.}\quad D = \max_{i=1}^{n}\,[F^*(x_i)-F(x)] = 0.566-0.420 = 0.146$$

$$\text{Log-normal C.D.F.}\quad D = \max_{i=1}^{n}\,[F^*(x_i)-F(x)] = 0.915-0.830 = 0.085$$

$$\text{Gamma}\quad\text{C.D.F.}\quad D = \max_{i=1}^{n}\,[F^*(x_i)-F(x)] = 0.900-0.835 = 0.065$$
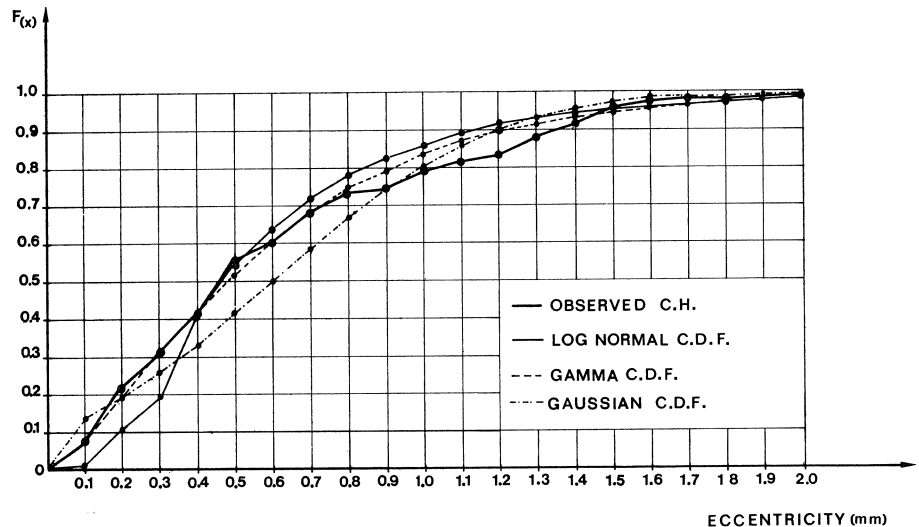
Fig. 7

The critical values of $\bar{D}$ are

$$\alpha = 0.10\qquad \bar{D} = 1.22/\sqrt{150} = 0.100$$

$$\alpha = 0.05\qquad \bar{D} = 1.36/\sqrt{150} = 0.111$$

$$\alpha = 0.01\qquad \bar{D} = 1.63/\sqrt{150} = 0.133$$

The log-normal and the Gamma C.D.F. cannot be rejected at the 10% level of significance. The Gamma-model is chosen for the eccentricity. The parameters of this model are

$$\left. \begin{array}{l} m = 0.5949 \text{ mm} \\ s \ = 0.4609 \text{ mm} \end{array} \right\} \rightarrow \begin{array}{l} \lambda = 2.798 \\ k = 1.663 \end{array}$$

5.2 Initial curvature

The initial curvature parameters f_0 has been determined for each column length 1 involved in the simulation. It is assumed that f_0 follows a Gaussian distribution function. In this case the Kolmogorov-Smirnov test is not used to check the validity of this assumption but the more refined method of "the moments" is used instead. This method is described in some detail in chapter 7. The following values are obtained for the critical parameters of this test.

	$l=1012$	$l=1380$	$l=1748$	$l=1932$	$l=2392$	$l=2944$
m	0.68	1.13	1.47	1.65	1.95	2.78
s	0.29	0.30	0.50	0.25	0.35	0.49
V_1	−1.40	−2.16	−4.91	−1.18	−0.60	1.84
V_2	−0.98	0.65	4.81	0.38	−0.92	1.09

The hypothesized Gaussian distribution function should be rejected if $V_1 > 3$ and $V_2 > 3$. This is only the case for $l = 1748$ mm ($\lambda = 95$). The hypothesized p.d.f. is accepted therefore for initial curvature. Fig. 8 shows the computed values of m.

Fig. 8

19
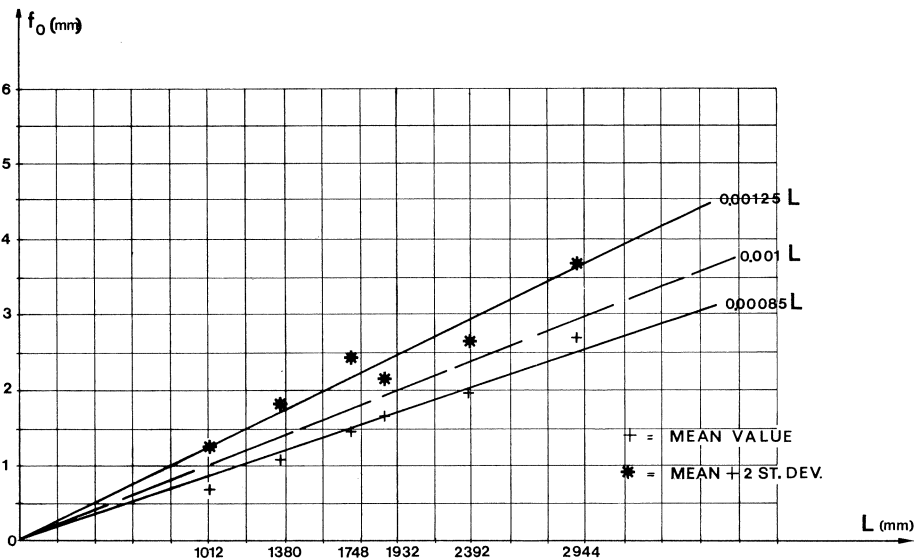
Also plotted are the values $m+2s$. It can be seen in this figure that the relations (l, m) and $(l, m+2s)$ can be approximated by straight lines. This indicates that the initial curvature parameter can be described independent of the column length through the value f_0/l. This parameter is considered in this paper; (Fig. 9) shows the histogram of f_0/l. From (Fig. 8) the following values are determined for the Gaussian model

$$m = 0.00085 \; l \; (\text{mm})$$

$$s \; = 0.00020 \; l \; (\text{mm})$$

Fig. 9

FREQUENCY

INITIAL CURVATURE $\quad f_0/L \cdot 10^{-3}$ mm
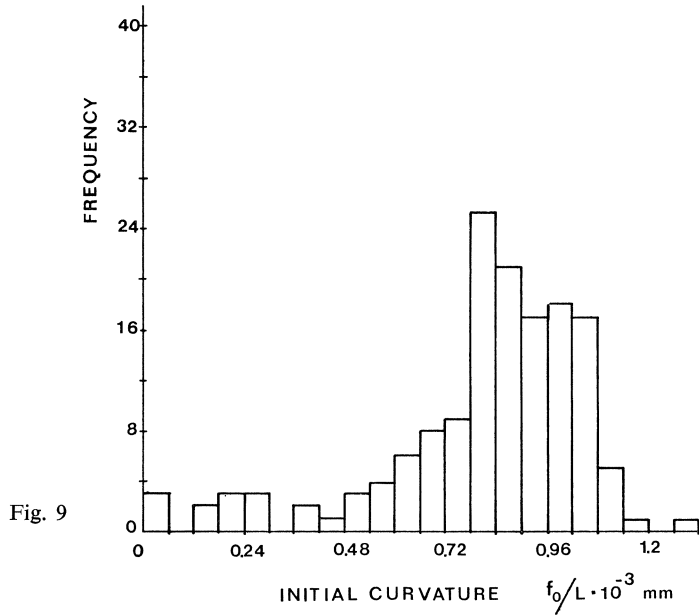
5.3 Area

The histogram of the area is given in (Fig. 10). The observed C.H. and the hypothesized Gaussian C.D.F. are shown in (Fig. 11). Preliminary computations indicate that hypothesizing an asymmetrical C.D.F. is not justified. The mean area is equal to $m = 2047.33$ mm^2. The standard deviation is equal to $s = 81.15$ mm^2.

The parameters k and λ of a Gamma C.D.F. are a function of m and s.

$$\frac{k}{\lambda} = m; \quad \frac{\sqrt{k}}{\lambda} = s$$

Substitution of the measured values of m and s into these formula gives

$$k = 636.51$$

$$\lambda = 0.3109$$

20

Fig. 10

Fig. 11
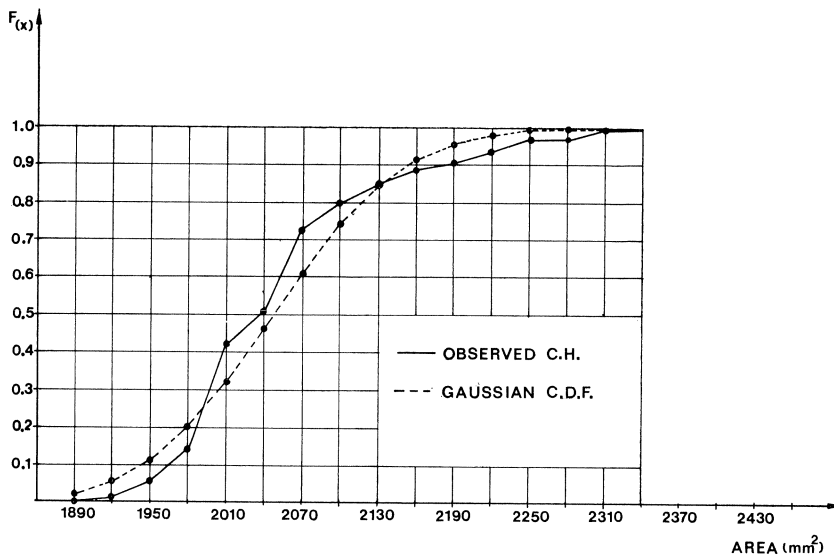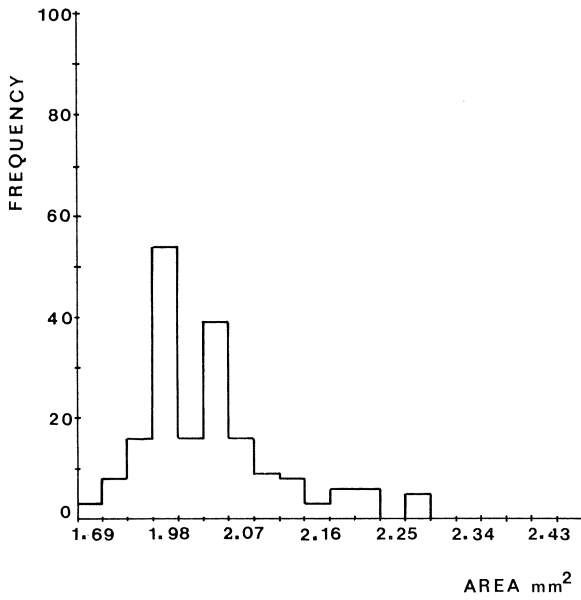
For large k-values the Gamma C.D.F. approaches a Gaussian C.D.F.

The latter is the only function, therefore, which has been investigated. The Kolmogorov-Smirnov test gives the following results.

$$D = \max_{i=1}^{n} [F^*(x_1) - F(x)] = 0.730 - 0.610 = 0.120$$

21

The critical values of $\bar{D}$ are

$$\alpha = 0.10 \qquad \bar{D} = 1.22/\sqrt{189} = 0.089$$

$$\alpha = 0.05 \qquad \bar{D} = 1.22/\sqrt{189} = 0.099$$

$$\alpha = 0.01 \qquad \bar{D} = 1.22/\sqrt{189} = 0.118$$

The Gaussian model cannot be rejected at the 1% level of significance, which is a rather questionable result. The Gaussian model is accepted, however, for reasons of convenience. The parameters of this model are

$$m = 2047.33 \text{ mm}^2$$

$$s = \quad 81.15 \text{ mm}^2$$

For the simulation procedure, the variation in the area is assumed to be a result of the variation in the flange thickness alone. The height, width and web thickness are assumed to be equal to the nominal values. The mean value and the standard deviation of the flange thickness are obtained from the following formulae

$$A = (h - 2e)a + 2be = (160 - 2e)5 + 2 \times 8.2e = 800 + 154e$$

mean value

$$m_e = \frac{\bar{A} - 800}{154} = 8.1 \text{ mm}$$

standard deviation

$$s_e = \frac{s_A}{154} = 0.527 \text{ mm.}$$

The parameters of the Gaussian model for the flange thickness, are

$$m = 8.1 \quad \text{mm}$$

$$s = 0.527 \text{ mm}$$

5.4 *Yield stress*

The yield stress has been determined from three different tests.

Euronorm	$m = 29.12 \text{ kgf/mm}^2$	$s = 2.04 \text{ kgf/mm}^2$
Strips	$m = 27.85 \text{ kgf/mm}^2$	$s = 3.17 \text{ kgf/mm}^2$
Stub-column	$m = 31.48 \text{ kgf/mm}^2$	$s = 2.65 \text{ kgf/mm}^2$

22
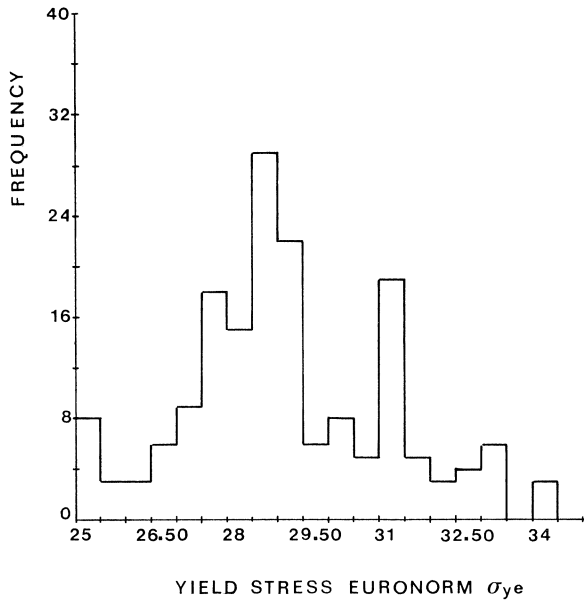
Fig. 12
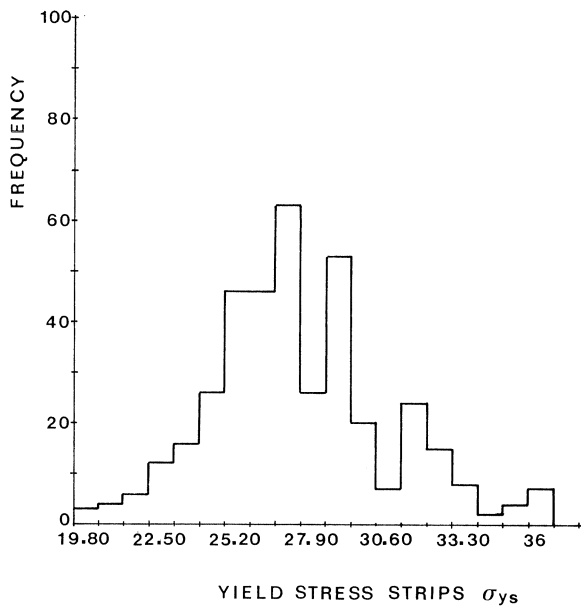
Fig. 13
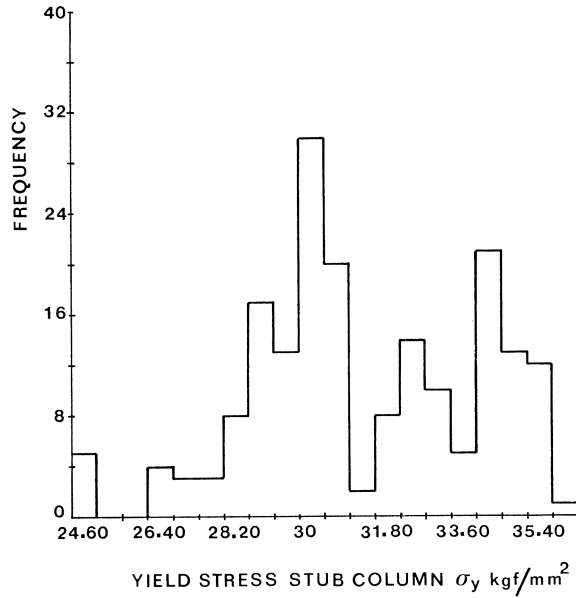
Fig. 14

The values obtained from the stub-column tests have been used in the simulation procedure because these values are the best measure for the yield stress in compression. This yield stress also determines the buckling load of a column. The histograms of the three yield stresses are shown in (Fig. 12, 13 and 14). The shape of the histograms suggests a symmetrical p.d.f. Fig. 15 shows the observed C.H. of the stub-column yield stress together with the hypothesized Gaussian. C.D.F. The Kolmogorov-Smirnov value D is equal to

$$D = \max_{i=1}^{n} [F^*(x_i) - F(x)] = 0.840 - 0.750 = 0.090$$

The critical value $\bar{D}$ is

$\alpha = 0.10 \qquad \bar{D} = 1.22/\sqrt{189} = 0.089$

$\alpha = 0.05 \qquad \bar{D} = 1.36/\sqrt{189} = 0.099$

$\alpha = 0.01 \qquad \bar{D} = 1.63/\sqrt{189} = 0.118$

The Gaussian model for the yield stress cannot be rejected at the 10% level of significance. The parameters of this model are

$m = 31.48 \ \text{kgf/mm}^2$

$s \ = \ 2.65 \ \text{kgf/mm}^2$

24
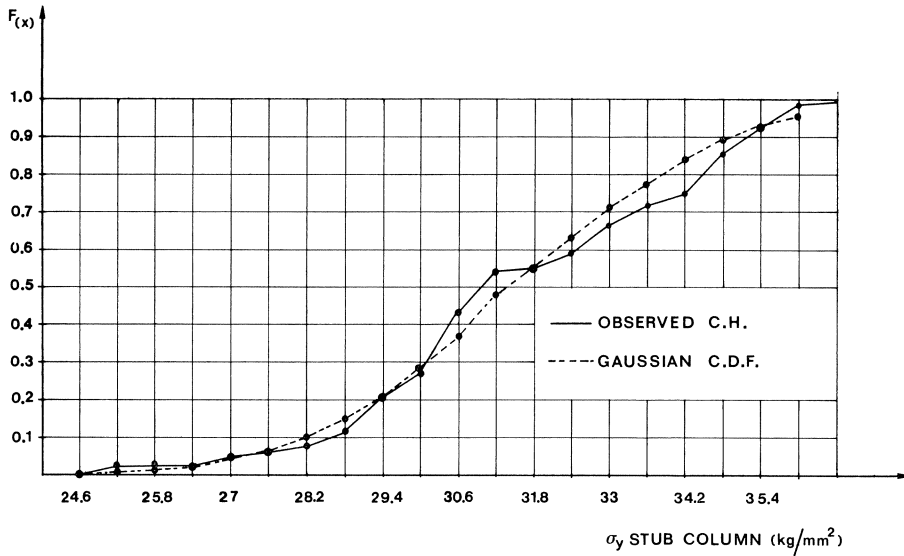
Fig. 15

5.5 Residual stress

The residual stresses provided most difficulties because no extensive residual stress-measurements have been done on IPE 160 sections. The distribution of the residual stresses is assumed to be parabolic in the flanges and constant in the web. As the parameter of this type of distribution the maximum compressive σ_r at the tip of the flange is chosen. Some stub-column tests were carried out in Belgium for which load-deformation diagrams were recorded [8]. From these diagrams the maximum residual stress can be estimated. Ten such diagrams are given. The maximum compressive residual stress is determined as a fraction of the yield stress.

$$\sigma_r = \alpha \sigma_y \rightarrow \alpha = \frac{\sigma_r}{\sigma_y}$$

A mean value $\alpha = 0.204$ and a standard deviation $s = 0.07$ are computed from the Belgian tests.

A value of $\alpha = 0.61$ is derived by Rokach. He performed a correlation analysis on the IPE 160 test results [9]. This value of α, however, must also account for the effect of the initial curvature. For the same sections Lenz arrives at a valus of $\alpha = 0.06$ [10].

Young suggests a general formula for the maximum compressive residual stress in I sections [11].

$$\sigma_r = 16.5 \left[1 - \frac{A_w}{1 \cdot 2 A_F} \right]$$

$A_w =$ web area
$A_F =$ flange area

25

For an IPE 160 a value of $\alpha = 0.238$ is computed. Schulz proposes a value $\alpha = 0.2$ for this type of section [12].

The residual stress parameter α is assumed to be Gaussian distributed [13]. The validity of this assumption cannot be tested due to lack of information. For the simulation procedure, a mean value $m = 0.20$ and a standard deviation $s = 0.05$ are adopted.

5.6 *Slenderness-ratio*

No variation is assumed in the slenderness-ratio λ. The length of each column has been determined with sufficient accuracy and no variation is assumed in the width of the column flanges.

For weak-axis bending, therefore, the radius of gyration is constant. The slenderness-ratio λ can thus not be treated as a random variable.

5.7 *Summary of the model parameters*

Random variable	Gamma C.D.F.		Gaussian C.D.F.	
	λ	k	m	s
Eccentricity (mm)	2.798	1.663	–	–
Initial curvature	–	–	$0.00085l$	$0.00020l$
Area (mm²)	–	–	2047.33	81.15
Flange thickness (mm)	–	–	8.1	0.527
Yield stress (kgf/mm²)	–	–	31.48	2.65
Residual stress (kgf/mm²)	–	–	$0.20\sigma_y$	$0.05\sigma_y$

6 Generating random numbers

Random numbers with a Gaussian or uniform probability density function can be generated directly on a digital computer. Standard procedures are generally available. Values of the variables for which a Gaussian model is assumed, have been obtained on a I.B.M. 1130 computer using the procedures RANDU and GAUSS. Generating random numbers with a Gamma p.d.f. proved more difficult. No standard procedure is available for the inversion of the incomplete Gamma function; therefore, a graphical method is used. First the Gamma C.D.F. is computed and intervals of equal probability (2.5%) are determined.

Next random numbers with a uniform p.d.f. are generated and they are assigned to these intervals. In this particular case, the random numbers lie between 0 and 10^5; they are assigned to each interval according to the following scheme

$$
\begin{array}{llll}
0-2.500 & \text{interval} & 1 & \text{representative value } x_1 \\
2501-5.000 & \text{interval} & 2 & \text{representative value } x_2 \\
5001-7.500 & \text{interval} & 3 & \text{representative value } x_3 \\
97501-100.000 & \text{interval} & 40 & \text{representative value } x_{40}
\end{array}
$$

Each interval i is represented by a single value x_i; x_i is defined as the mean value of the two boundary values of interval i. This is not correct. Theoretically x_i should be defined as the center of gravity of the area under the C.D.F. between the two boundary values. The relatively large number of intervals, however, assures that the error will be very small if the mean is considered instead of the center of gravity. The last interval must be treated with special care, because $x \to \infty$. The largest observed value of the eccentricity is chosen as the representative value of this interval. As an example of the above-mentioned procedure, let a random number 11533 be generated. This value corresponds to interval 5 and therefore to x_5. This value of x is assigned to the eccentricity. It is obvious that a Gamma p.d.f. can be approximated with increasing accuracy by raising the number of intervals.

For each variable considered in the column simulation, a series of 1000 random numbers has been generated. There is no need for a sophisticated procedure to combine the variables because the variables are assumed to be uncorrelated. One must beware, however, of sequential effects in the random numbers. A digital computer generates random numbers according to a numerical procedure, very often the Fibonacci-method is used. Consequently, each time the random number generator is started, the same sequence of number appears. If the variables are combined according to their rank-number, they will be strongly correlated: a large value of the yield stress will be combined with a large value of the initial curvature, eccentricity etc. For this reason more than the required random numbers have been generated and each column variable has been selected at random from these numbers.

The combinations of variables obtained in this way are used as input for the computer programme described briefly in chapter 3.

7 Results

Columns of various lengths have been examined. The corresponding slenderness-ratios are $\lambda = 55$, 75, 95, 105, 130 and 160. At each slenderness-ratio experimental results are available which can be compared with the simulated buckling stresses. Each group of experimental buckling stresses had a significant influence on the shape and position of the experimental buckling curve.

A total number of 120 columns has been simulated on an I.B.M. 360/65 digital computer; 20 columns at each slenderness-ratio.

The results of the computations are given in tables I through VI. The combinations of variables which are assigned to each column are also given in these tables. Buckling stresses are computed for the nominal area as well as for the real area. For each section the real area is determined from the value of the flange thickness e. These buckling stresses are also given in tables I through VI. Columns with a yield stress less than the guaranteed value of 24 kgf/mm^2, have not been included in the computations.

The probability density-function of the buckling stress is estimated at each slenderness-ratio λ. Jaquet has shown that the experimental buckling stresses are

Gaussian distributed [14]. He arrived at this conclusion by applying the method of the central-moments to the test results. This method has been described in detail by Fisher [15].

The same method is applied to check whether the simulated buckling stresses are Gaussian distributed. A brief discussion of this method is given below. Consider a variate x and a random sample of size n, drawn from the population of x. The sums of powers of deviations from the mean are computed.

$$m = \frac{\Sigma x}{n}$$

$$s_2 = \Sigma(x-m)^2 \rightarrow k_2 = s_2/(n-1)$$

$$s_3 = \Sigma(x-m)^3 \rightarrow k_3 = ns_3/(n-1)(n-2)$$

$$s_4 = \Sigma(x-m)^4 \rightarrow k_4 = n[(n+1)s_4 - 3(n-1)s_2^2/n]/[(n-1)(n-2)(n-3)]$$

The two simplest measures of departure from normality are those dependent from the statistics of the 3rd and 4th degree, defined as

$$g_1 = k_3/k_2^{3/2} \qquad g_2 = k_4/k_2^2$$

If the variate x is Gaussian distributed then g_1 and g_2 are also Gaussian distributed. The sampling variances of g_1 and g_2 are

$$\hat{s}_1^2 = 6n(n-1)/(n-2)(n+1)(n+3)$$

$$\hat{s}_2^2 = 24n(n-1)^2/(n-3)(n-2)(n+3)(n+5)$$

Finally

$$V_1 = \frac{g_1}{\hat{s}_1} \quad \text{and} \quad V_2 = \frac{g_2}{\hat{s}_2}$$

are computed. For a perfectly Gaussian distributed variate x, the values of V_1 and V_2 are equal to zero. For each symmetrical p.d.f. $V_1 = 0$. A positive value of V_1 indicates a positive skewness whereas a negative value of V_2 indicates a negative skewness. V_2 is a coefficient of kurtosis (flatness).

A positive value of V_2 means that the p.d.f. is more filled out than a Gaussian p.d.f. whereas a negative value of V_2 means that the p.d.f. is more pointed that a Gaussian p.d.f.

The observed values of V_1 and V_2 determine whether the hypothesized Gaussian p.d.f. is to be rejected. Jaquet suggests to reject the hypothesis if V_1 and V_2 are greater than 3. For values greater than 2, the hypothesis should be reconsidered carefully.

The computed value of V_1 and V_2 are given in the tables below. The values have been determined for the nominal area as well as for the real area.

NOMINAL AREA

	55	75	95	105	130	160
m	26.60	22.09	16.58	14.74	11.22	7.73
s	2.60	1.96	1.71	1.65	0.92	0.62
V_1	− 1.44	− 0.91	− 0.22	0.88	0.08	−0.19
V_2	0.40	0.12	− 0.56	− 0.11	− 0.14	−1.13

REAL AREA

	55	75	95	105	130	160
m	26.04	21.39	16.60	14.59	10.86	7.63
s	1.92	1.37	1.40	1.19	0.59	0.33
V_1	− 1.80	0.43	− 0.05	0.29	− 0.14	−0.23
V_2	0.45	1.07	0.14	0.05	1.77	−0.50

All values are shown to be less than 1.8, most of them being less than 1.0. There is no reason to reject the hypothesis that the buckling stresses are Gaussian distributed. Consequently the characteristic buckling stress σ_{CR}^{*} can be computed as

$$\sigma_{CR}^{*} = m - 2s$$

The values of σ_{CR}^{*} at each slenderness-ratio are given in the next tables. The simulated values and the corresponding experimental values of σ_{CR}^{*} are given.

NOMINAL AREA

		55	75	95	105	130	160
	m	26.60	22.09	16.58	14.74	11.22	7.73
SIMULATION	s	2.60	1.96	1.71	1.65	0.92	0.62
	$m-2s$	21.40	18.17	13.16	11.44	9.38	6.59
	m	27.90	23.15	18.70	15.27	11.35	7.44
EXPERIMENT	s	2.73	2.45	1.46	1.23	1.00	0.56
	$m-2s$	22.40	18.29	15.78	12.81	9.35	6.32

REAL AREA

		55	75	95	105	130	160
	m	26.04	21.39	16.60	14.59	10.86	7.66
SIMULATION	s	1.92	1.37	1.40	1.19	0.59	0.33
	$m-2s$	22.20	18.65	13.80	12.21	9.68	7.00
	m	27.48	22.81	18.45	15.06	11.14	7.34
EXPERIMENT	s	2.48	2.05	1.21	1.00	0.73	0.36
	$m-2s$	22.52	18.71	16.03	13.06	9.68	6.62
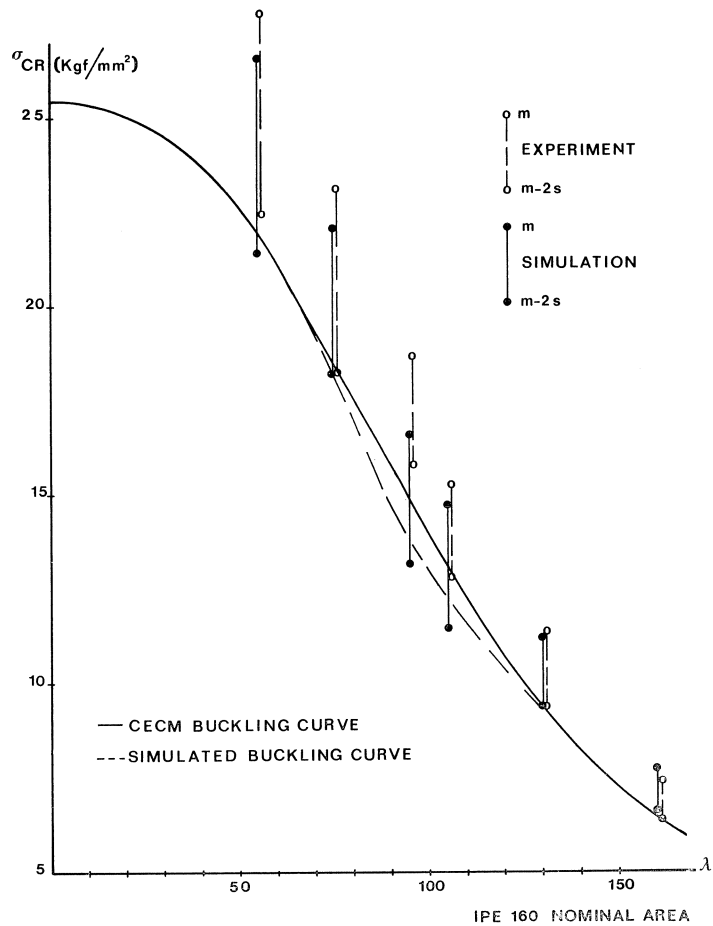
Fig. 16

These results are also shown graphically in (Figs 16 and 17). A good agreement is found between the simulated buckling stresses and the experimental buckling stresses at slenderness-ratios $\lambda = 55$, 75, 130 and 160. At slenderness-ratios $\lambda = 95$ and 105 the simulated buckling stresses deviate significantly from the experimental buckling stresses The maximum deviation is 17% ($\lambda = 95$, nom. area).

The dotted lines, in (Figs. 16 and 17), correspond to a buckling curve fitted to the simulated buckling stresses (real area).

The discrepancies between both curves at $\lambda = 95$ and $\lambda = 105$ cannot be traced to exceptionally large imperfections or unfavourable mechanical properties. Confidence intervals have been determined for the means and the standard deviations. These intervals are important because the means and the standard deviations are computed from samples of limited size.

30
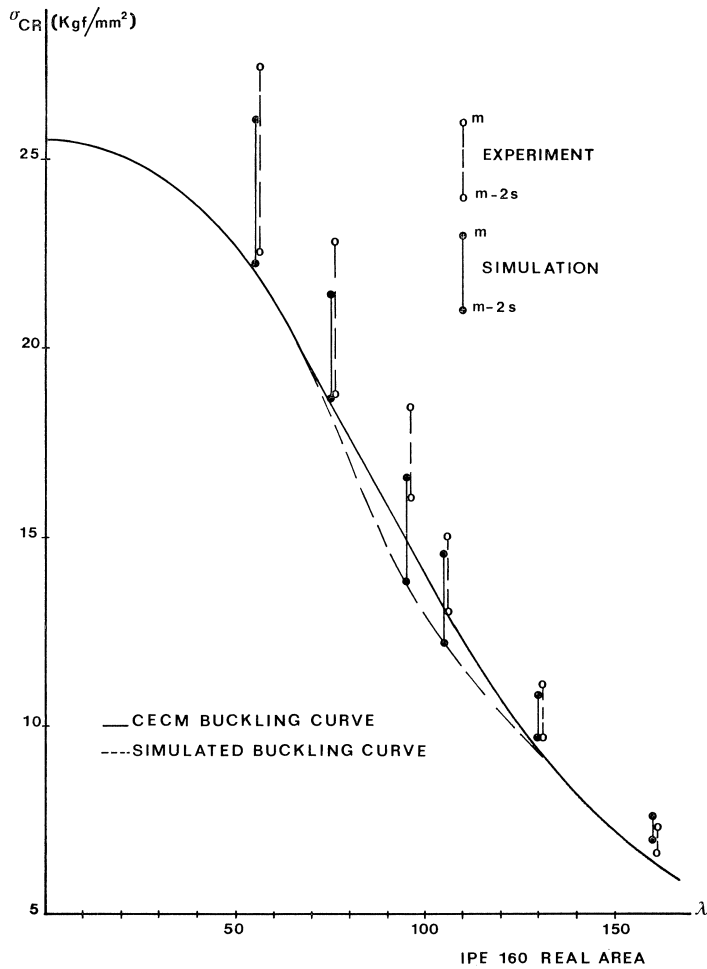
Fig. 17

Let m and s be the sample estimates, based on a random sample of size n; the confidence interval of the mean is

$$m'' = m - t \cdot \frac{s}{\sqrt{n}} < \overline{m} < m' = m + t \cdot \frac{s}{\sqrt{n}}$$

where $\overline{m}$ is the population mean and t possesses a Student's t distribution with $n-1$ degrees of freedom.

The value of t is chosen to correspond to a 98% confidence interval. The bounds of this interval are given in the table below.

The confidence intervals of the simulated mean stress and the experimental mean stress are shown in (Figs. 18 and 19).
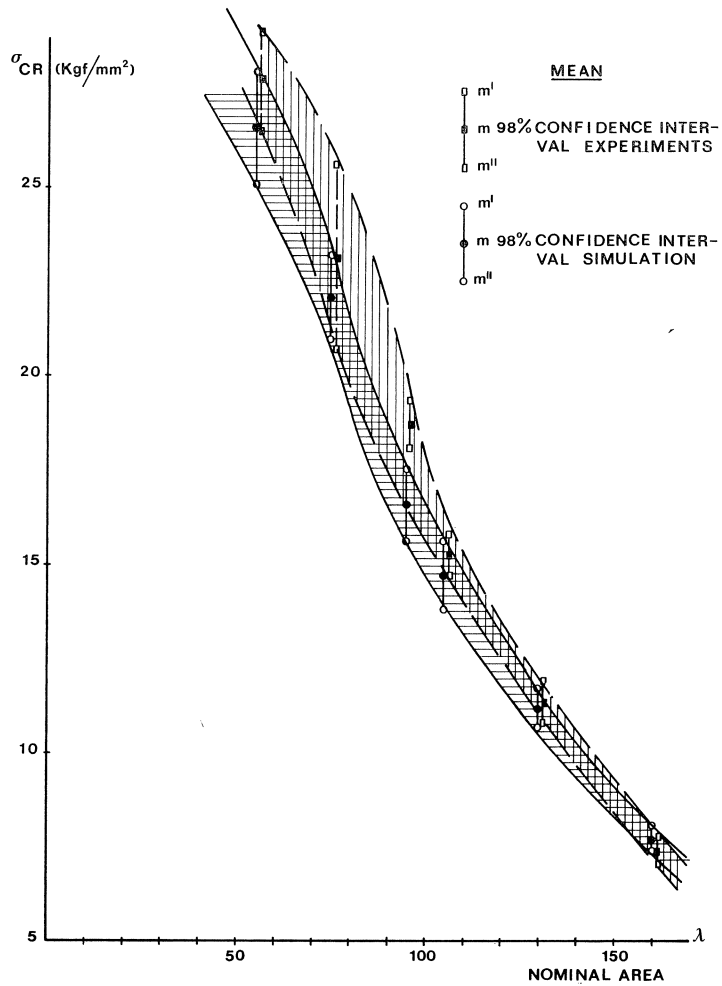
Fig. 18

CONFIDENCE LIMITS OF THE MEAN 98%

		55	75	95	105	130	160
	m	26.60	22.09	16.58	14.74	11.22	7.73
NOMINAL AREA	m'	28.12	23.20	17.55	15.68	11.74	8.08
	m''	25.08	20.98	15.61	13.80	10.70	7.38
	m	26.04	21.39	16.60	14.59	10.86	7.66
REAL AREA	m'	27.16	22.17	17.39	15.26	11.19	7.84
	m''	24.92	20.61	15.81	13.92	10.53	7.48

It can be seen that the experimental mean stresses are almost systematically greater than the simulated stresses, except at $\lambda = 160$. The confidence intervals, however,
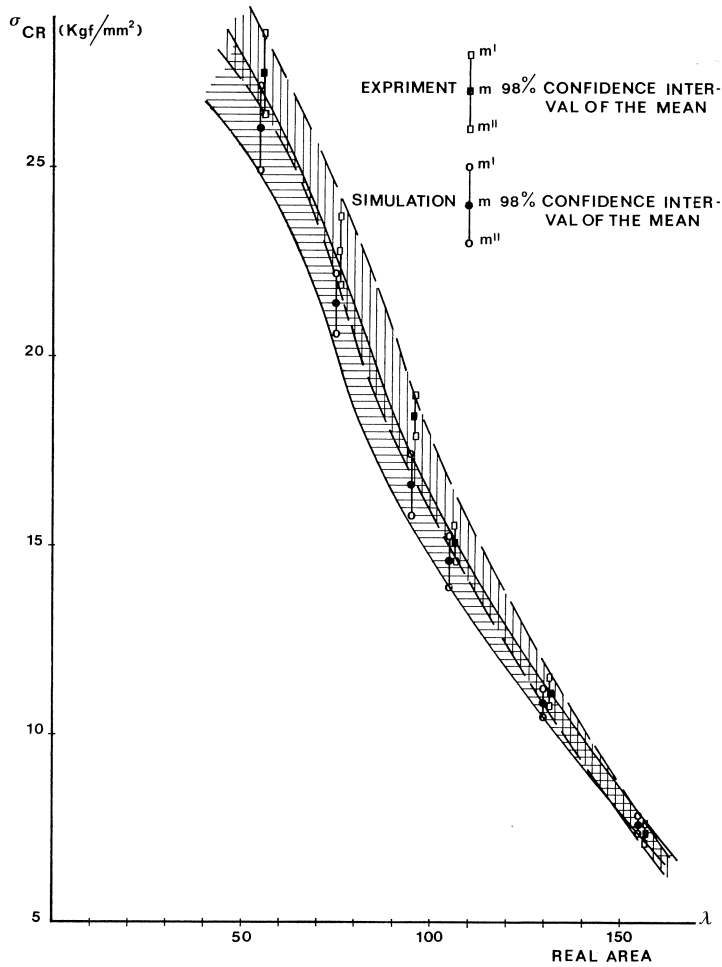
Fig. 19

overlap slightly. The confidence interval of the mean stress obtained from the nominal area is somewhat wider than the confidence interval which corresponds to the real area. The reason is that dividing the buckling loads by the real area eliminates to some extend the influence of the flange thickness. A small flange thickness corresponds to a smaller buckling load but also to a smaller area, and vica-versa. Consequently, the scatter in the buckling stresses will be reduced.

The confidence interval of the standard deviation s has been computed by observing that the quantity $\Sigma(x_i - m)^2/s^2$ possesses a Ψ^2 distribution with $n-1$ degrees of freedom.

The confidence interval is given by

33

$$s'' = \sqrt{\frac{\Sigma(x_i-m)^2}{\Psi_2^2}} < s < s' = \sqrt{\frac{\Sigma(x_i-m)^2}{\Psi_1^2}}$$

Ψ_1 and Ψ_2 are chosen such that they correspond to 5% and 95% confidence limits. The computed values are given in the table below.

CONFIDENCE LIMITS OF THE STANDARD DEVIATION 90%

		55	75	95	105	130	160
	s	2.60	1.96	1.71	1.65	0.92	0.62
NOMINAL AREA	s'	3.60	2.69	2.34	2.26	1.26	0.85
	s''	2.05	1.56	1.36	1.31	0.73	0.49
	s	1.92	1.37	1.40	1.19	0.59	0.33
REAL AREA	s'	2.66	1.88	1.92	1.63	0.81	0.45
	s''	1.52	1.09	1.11	0.95	0.47	0.26

8   Conclusions

It has been demonstrated in this paper, that the distribution function of buckling stresses can be derived theoretically. A buckling curve which corresponds to a constant probability of failure can be determined from the distribution functions at the various slenderness-ratios. The computed buckling curve is in reasonable agreement with the experimental buckling curve. Deviations between the two curves are observed at slenderness-ratios $\lambda = 95$ and $\lambda = 105$. It has been pointed out by other investigations that the effect of imperfections and/or mechanical properties is most pronounced at slenderness-ratios $\lambda = 90 - 100$ [2]. One of the assumptions in the discussed simulation procedure is that all variables are uncorrelated. There is no reason to reject this assumption except for the initial curvature and the residual stresses. It is believed that some correlation exists between those two variables; consequently, the buckling stresses may be affected unfavourably.

Application of the described procedure to sections other than the IPE 160 is a rather simple matter. The distribution functions of the variables are not expected to change in character; the parameters of these functions will vary. These values can be determined by relatively simple and inexpensive measurements. Once buckling curves have been obtained for various sections, the usefullness of multiple column-curves can be decided upon. Adoption of multiple column-curves can only be justified if significant differences are shown to exist between probabilistic column curves. The buckling curves which are derived by means of the discussed procedure, are in the right format to be used as a "strength function" in load factor design. This is generally not true for most theoretically derived buckling curves.

References

1. CONSTRUCTION METALLIQUE, No. 3, Septembre, 1970.
2. BATTERMAN, R. H. and B. G. JOHNSTON, Behavior and maximum strength of metal columns. Proc. A.S.C.E., April, 1967.
3. STUSSI, F., Grundlagen des Stahlbaues. Springer-Verlag, Berlin, New York, 1971.
4. BEER, H. and G. SCHULZ, Bases théoriques des courbes européennes de flambement (Principles of the European buckling curves). Construction Métallique, No. 3, Septembre, 1970.
5. LOOF, H. W., Recherche par la statistique mathématique des relations pouvant exister entre les résultats d'essais de flambement et les paramètres intervenant dans le phénomène. (A statistical analysis of the relations between the column variables and the buckling load). DOC. Committee 8, ECCS.
6. SCHOR, R. J., Private communication with prof. H. Beer.
7. BENJAMIN, J. R. and C. A. CORNELL, Probability, statistics and decision for civil engineers. McGraw-Hill Book Co., 1970.
8. E.C.C.S. Committee 8. Essais sur tronçons courts. (Tests on stub columns). January, 1966.
9. ROKACH, A. J., A statistical study of the steel columns. M.I.T., Report R70-60, September, 1970.
10. LENZ, J. C., Reliability based design rules for column buckling. Washington University, Sever Institute of Technology, January, 1972.
11. YOUNG, B. W., Residual stresses in hot-rolled sections. University of Cambridge, Department of Engineering, CUED/C-STRUCT/TR 8 (1971).
12. SCHULZ, G., Die Traglastberechnung von planmässig mittig belasteten Druckstäben aus Baustahl unter Berücksichtigung von geometrischen und strukturellen Imperfektionen. Dissertation, Graz, Juni, 1968.
13. BEEDLE, L. S. and L. TALL, Basic column strength. A.S.C.E. J. Struct. Div. 86, No. ST 7, July, 1960.
14. JAQUET, J., Essais de flambement et exploitation statistique. (Buckling tests and their statistical analysis). Construction Métallique, No. 3, Septembre, 1970.
15. FISHER, R. S., Statistical methods for research workers. Oliver and Boyd, Edinburgh, 1954.

Table I $\lambda = 55$

Nr.	L (mm)	σ_y (kgf/ mm²)	e_0 (mm)	f_0 (mm)	a (mm)	b (mm)	e (mm)	h (mm)	α	P_{CR} (kgf)	σ_{CRR} (kgf/ mm²)	σ_{CRN} (kgf/ mm²)	Nr.
1	506	34.16	0.83	1.04	5	82	8.42	160	0.1260	56586	26.99	28.15	1
2	506	23.36	0.55	0.88	5	82	8.39	160	0.2233	41971			2
3	506	27.85	1.28	1.07	5	82	7.18	160	0.2581	40659	21.34	20.23	3
4	506	31.67	0.44	0.81	5	82	8.74	160	0.1303	57751	26.91	28.73	4
5	506	34.85	0.50	0.90	5	82	8.04	160	0.2401	55752	27.35	27.74	5
6	506	34.70	1.28	0.73	5	82	8.02	160	0.2374	52886	25.99	26.31	6
7	506	31.24	0.23	0.72	5	82	7.85	160	0.1221	54492	27.13	27.11	7
8	506	32.24	0.52	0.86	5	82	8.09	160	0.0944	55397	27.08	27.56	8
9	506	30.29	0.64	0.95	5	82	7.67	160	0.1541	48787	24.63	24.27	9
10	506	30.15	1.42	0.79	5	82	8.16	160	0.2014	47209	22.95	23.49	10
11	506	29.34	0.42	1.19	5	82	8.00	160	0.1862	50294	24.75	25.02	11
12	506	30.52	0.83	0.92	5	82	8.24	160	0.1584	51741	25.00	25.74	12
13	506	31.04	0.21	0.81	5	82	7.81	160	0.2682	57418	28.67	28.57	13
14	506	36.19	0.61	0.65	5	82	8.31	160	0.2155	57917	27.85	28.81	14
15	506	35.39	0.52	0.44	5	82	7.10	160	0.2002	53026	28.00	26.38	15
16	506	33.92	0.16	0.97	5	82	8.91	160	0.2225	57686	26.56	28.70	16
17	506	31.78	0.16	1.06	5	82	9.01	160	0.2323	60876	27.83	30.29	17
18	506	34.29	1.42	0.70	5	82	8.46	160	0.2295	50175	23.86	24.96	18
19	506	30.83	0.58	0.69	5	82	9.35	160	0.1643	60453	26.99	30.07	19
20	506	32.01	0.69	0.63	5	82	6.95	160	0.1366	46680	24.96	23.22	20

Table II $\lambda = 75$

Nr.	L (mm)	σ_y (kgf/ mm²)	e_0 (mm)	f_0 (mm)	a (mm)	b (mm)	c (mm)	h (mm)	α	P_{CR} (kgf)	σ_{CRR} (kgf/ mm²)	σ_{CRN} (kgf/ mm²)	Nr.
21	690	31.54	0.71	0.81	5	82	7.76	160	0.2020	42930	21.52	21.36	21
22	690	31.31	0.79	1.41	5	82	8.06	160	0.1430	42377	20.76	21.83	22
23	690	30.50	0.25	1.39	5	82	7.71	160	0.1715	42151	21.21	20.97	23
24	690	31.68	0.19	0.76	5	82	8.27	160	0.2375	47276	22.80	23.52	24
25	690	29.55	0.25	0.88	5	82	8.17	160	0.1411	45540	22.13	22.66	25
26	690	32.05	0.21	1.21	5	82	9.00	160	0.2321	49174	22.49	24.46	26
27	690	31.24	0.55	0.93	5	82	9.17	160	0.2106	49090	22.19	24.42	27
28	690	32.42	0.79	1.12	5	82	8.15	160	0.1766	44073	21.45	21.93	28
29	690	32.94	0.07	1.52	5	82	9.11	160	0.2801	48933	22.21	24.34	29
30	690	30.15	0.64	1.02	5	82	8.36	160	0.2211	43319	20.75	21.55	30
31	690	31.99	0.55	1.56	5	82	7.47	160	0.2497	39357	20.18	19.58	31
32	690	30.52	0.88	1.46	5	82	6.98	160	0.2657	35125	18.73	17.48	32
33	690	28.39	0.07	1.61	5	82	9.00	160	0.2192	44460	20.34	22.12	33
34	690	30.89	0.07	1.64	5	82	8.77	160	0.1602	47407	22.04	23.59	34
35	690	29.43	0.31	1.08	5	82	7.89	160	0.1887	40141	19.92	19.97	35
36	690	31.27	0.29	1.55	5	82	8.45	160	0.1047	46621	22.19	23.19	36
37	690	29.13	0.27	0.84	5	82	7.83	160	0.1582	43848	21.86	21.81	37
38	690	36.94	0.40	0.90	5	82	8.13	160	0.1993	50870	24.79	25.31	38
39	690	28.18	0.83	1.16	5	82	8.30	160	0.2278	39861	19.80	19.83	39
40	690	29.36	0.27	1.08	5	82	8.86	160	0.2438	45613	21.07	22.69	40

Table III $\lambda = 95$

Nr.	L (mm)	σ_y (kgf/mm²)	e_0 (mm)	f_0 (mm)	a (mm)	b (mm)	c (mm)	h (mm)	α	P_{CR} (kgf)	σ_{CRR} (kgf/mm²)	σ_{CRN} (kgf/mm²)	Nr.
41	874	34.54	0.58	1.28	5	82	7.82	160	0.1491	36172	18.05	18.00	41
42	874	39.03	1.28	1.75	5	82	7.64	160	0.2088	33020	16.71	16.43	42
43	874	34.91	1.07	1.07	5	82	7.35	160	0.1561	33186	17.18	16.51	43
44	874	30.13	0.25	1.69	5	82	7.45	160	0.1909	31729	16.29	15.79	44
45	874	29.98	0.42	1.55	5	82	7.95	160	0.2631	32727	16.17	16.28	45
46	874	29.17	0.42	1.31	5	82	7.79	160	0.1729	33545	16.78	16.69	46
47	874	27.70	1.28	2.04	5	82	7.56	160	0.2701	26730	13.67	13.30	47
48	874	28.22	0.14	1.63	5	82	8.65	160	0.2549	35072	16.45	17.45	48
49	874	30.73	1.28	1.82	5	82	7.04	160	0.1772	27868	14.79	13.86	49
50	874	29.92	1.07	1.94	5	82	7.94	160	0.2870	29699	14.68	14.78	50
51	874	28.45	0.16	1.61	5	82	7.12	160	0.1842	30554	16.11	15.20	51
52	874	34.27	0.36	1.21	5	82	8.28	160	0.2690	37220	17.94	18.52	52
53	874	26.17	0.09	1.40	5	82	8.77	160	0.1413	36645	17.04	18.23	53
54	874	30.66	0.23	0.80	5	82	8.09	160	0.1510	38397	18.77	19.10	54
55	874	26.54	0.42	1.19	5	82	8.32	160	0.1983	33961	16.32	16.90	55
56	874	32.36	0.07	1.47	5	82	7.90	160	0.1831	36275	17.99	18.05	56
57	874	34.87	1.07	1.60	5	82	7.34	160	0.2053	31289	16.21	15.57	57
58	874	31.41	0.44	1.78	5	82	8.23	160	0.2651	33596	16.25	16.71	58
59	874	32.59	1.64	1.45	5	82	7.41	160	0.2124	29532	15.23	14.69	59
60	874	30.46	0.14	0.70	5	82	8.04	160	0.1471	39469	19.37	19.64	60

Table IV $\lambda = 105$

Nr.	L (mm)	σ_y (kgf/mm²)	e_0 (mm)	f_0 (mm)	a (mm)	b (mm)	c (mm)	h (mm)	α	P_{CR} (kgf)	σ_{CRR} (kgf/mm²)	σ_{CRN} (kgf/mm²)	Nr.
61	966	34.35	2.00	1.28	5	82	7.70	160	0.1532	27861	14.03	13.86	61
62	966	31.55	0.38	1.30	5	82	6.94	160	0.1567	27964	14.96	13.91	62
63	966	33.40	0.46	1.24	5	82	8.69	160	0.1477	35256	16.49	17.54	63
64	966	31.93	0.58	1.83	5	82	8.73	160	0.2262	31934	14.89	15.89	64
65	966	27.14	1.07	1.95	5	82	8.64	160	0.2422	28005	13.14	13.93	65
66	966	29.65	0.36	1.99	5	82	7.88	160	0.2458	28225	14.02	14.04	66
67	966	31.49	2.00	1.91	5	82	7.52	160	0.2368	24807	12.97	12.34	67
68	966	30.02	0.52	1.76	5	82	7.03	160	0.2153	25920	13.77	12.90	68
69	966	33.19	0.75	1.49	5	82	7.99	160	0.1813	30607	15.07	15.23	69
70	966	35.70	0.07	1.51	5	82	8.29	160	0.1848	34468	16.60	17.15	70
71	966	29.59	1.42	2.22	5	82	7.40	160	0.2758	24003	12.38	11.94	71
72	966	30.77	0.75	1.28	5	82	8.49	160	0.1543	32212	15.28	16.03	72
73	966	33.94	0.50	2.18	5	82	8.41	160	0.2704	30570	14.59	15.21	73
74	966	33.79	0.42	1.82	5	82	8.18	160	0.2239	31199	15.15	15.52	74
75	966	32.98	0.36	2.12	5	82	7.82	160	0.2649	28934	14.44	14.40	75
76	966	31.51	0.16	1.20	5	82	8.91	160	0.1434	36597	16.85	18.21	76
77	966	32.03	0.29	2.09	5	82	8.29	160	0.2594	30308	14.59	15.08	77
78	966	29.24	0.52	1.35	5	82	7.54	160	0.1629	28758	14.66	14.31	78
79	966	31.08	0.25	1.66	5	82	7.18	160	0.2040	27797	14.59	13.83	79
80	966	32.26	0.70	2.26	5	82	7.74	160	0.2825	29292	13.70	13.58	80

Table V $\lambda = 130$

Nr.	L (mm)	σ_y (kgf/mm²)	e_0 (mm)	f_0 (mm)	a (mm)	b (mm)	c (mm)	h (mm)	α	P_{CR} (kgf)	σ_{CRR} (kgf/mm²)	σ_{CRN} (kgf/mm²)	Nr.
81	1196	34.67	0.09	1.71	5	82	8.65	160	0.2334	24992	11.72	12.43	81
82	1196	33.53	0.71	2.75	5	82	7.30	160	0.1932	19399	10.08	9.65	82
83	1196	31.73	0.64	1.29	5	82	7.93	160	0.2405	22183	10.98	11.04	83
84	1196	29.27	1.07	1.63	5	82	8.43	160	0.1752	22378	10.67	11.33	84
85	1196	31.44	0.94	1.84	5	82	7.74	160	0.0975	21288	10.69	10.59	85
86	1196	32.95	0.71	2.90	5	82	8.50	160	0.2073	22198	10.53	11.04	86
87	1196	31.15	0.23	2.37	5	82	8.08	160	0.2045	21985	10.75	10.94	87
88	1196	33.99	0.94	2.23	5	82	8.58	160	0.1393	23315	10.99	11.60	88
89	1196	33.51	0.44	2.44	5	82	8.42	160	0.1116	23390	11.16	11.64	89
90	1196	32.37	1.00	1.10	5	82	8.65	160	0.2213	24011	11.26	11.95	90
91	1196	33.22	0.23	1.08	5	82	8.75	160	0.1686	26259	12.23	13.06	91
92	1196	36.06	0.40	2.37	5	82	8.20	160	0.2034	22833	11.07	11.36	92
93	1196	27.63	0.07	3.06	5	82	8.04	160	0.1756	20820	10.22	10.36	93
94	1196	34.44	0.19	2.20	5	82	7.22	160	0.1854	20545	10.75	10.22	94
95	1196	29.99	0.58	1.70	5	82	7.85	160	0.2327	21292	10.60	10.59	95
96	1196	35.48	0.71	2.51	5	82	8.35	160	0.2174	22511	10.79	11.20	96
97	1196	32.35	0.46	2.25	5	82	9.24	160	0.1897	25153	11.36	12.56	97
98	1196	31.21	0.64	1.37	5	82	8.42	160	0.2495	23322	11.12	11.60	98
99	1196	29.41	0.38	2.78	5	82	9.05	160	0.1467	23773	10.84	11.83	99
100	1196	26.95	0.61	3.11	5	82	7.97	160	0.2815	19144	9.44	9.52	100

Table VI $\lambda = 160$

Nr.	L (mm)	σ_y (kgf/mm²)	e_0 (mm)	f_0 (mm)	a (mm)	b (mm)	c (mm)	h (mm)	α	P_{CR} (kgf)	σ_{CRR} (kgf/mm²)	σ_{CRN} (kgf/mm²)	Nr.
101	1472	35.37	0.03	2.22	5	82	8.26	160	0.1567	16683	8.05	8.30	101
102	1472	30.26	0.09	1.20	5	82	6.98	160	0.1977	14276	7.61	7.10	102
103	1472	32.43	1.28	1.86	5	82	8.73	160	0.1762	16641	7.76	8.28	103
104	1472	33.95	0.27	1.74	5	82	8.76	160	0.2422	17512	8.15	8.71	104
105	1472	34.80	0.61	2.67	5	82	7.09	160	0.1957	13707	7.25	6.82	105
106	1472	32.33	0.42	2.28	5	82	8.44	160	0.1368	16573	7.89	8.25	106
107	1472	29.21	0.03	1.96	5	82	7.56	160	0.2153	14980	7.63	7.45	107
108	1472	33.37	0.50	1.82	5	82	8.65	160	0.2313	17055	8.00	8.49	108
109	1472	31.57	1.64	0.75	5	82	8.03	160	0.1848	15609	7.66	7.77	109
110	1472	29.10	0.31	2.13	5	82	8.33	160	0.1758	16221	7.79	8.07	110
111	1472	36.58	0.33	2.19	5	82	7.97	160	0.2043	15886	7.84	7.90	111
112	1472	32.79	0.75	2.07	5	82	7.48	160	0.2704	14326	7.34	7.13	112
113	1472	33.64	0.03	1.23	5	82	8.44	160	0.2239	17297	8.24	8.61	113
114	1472	33.82	0.64	3.21	5	82	7.16	160	0.1649	13626	7.16	6.78	114
115	1472	33.35	1.07	3.24	5	82	8.38	160	0.1934	15519	7.42	7.72	115
116	1472	32.21	1.28	3.14	5	82	7.36	160	0.1594	13589	7.03	6.76	116
117	1472	33.06	0.88	2.28	5	82	7.80	160	0.1129	15139	7.56	7.53	117
118	1472	27.94	0.42	1.89	5	82	7.57	160	0.2040	14696	7.48	7.31	118
119	1472	27.47	0.64	1.32	5	82	8.27	160	0.1825	16205	7.81	8.06	119
120	1472	31.63	0.09	2.40	5	82	7.77	160	0.2985	15029	7.53	7.48	120